J. Biochem. 120, 505-510 (1996)

The Crystal Structure of Lipase II from *Rhizopus niveus* at 2.2 Å Resolution

Mitsutaka Kohno,*[,1] Jiro Funatsu,* Bunzo Mikami,† Wataru Kugimiya,* Takaharu Matsuo,* and Yuhei Morita*

**Central Research Institute Tsukuba R&D Center, Fuji Oil Co., Ltd., 4-3 Kinunodai, Yawara, Tsukuba-gun, Ibaraki 300-24; and †Research Institute for Food Science, Kyoto University, Uji, Kyoto 611*

Received for publication, March 6, 1996

The crystal and molecular structure of Lipase II from *Rhizopus niveus* was analyzed using X-ray single crystal diffraction data at a resolution of 2.2 Å. The structure was refined to an *R*-factor of 0.19 for all available data. This lipase was purified and crystallized as Lipase I, which contains two polypeptide chains combined through non-covalent interaction. However, during crystal growth, Lipase I was converted to Lipase II, which consists of a single polypeptide chain of 269 amino acid residues, by limited proteolysis. The structure of Lipase II shows a typical α/β hydrolase fold containing the so-called nucleophilic elbow. The catalytic center of this enzyme is analogous to those of other neutral lipases and serine proteases. This catalytic center is sheltered by an α-helix lid, which appears in neutral lipases, opening the active site at the oil-water interface.

Key words: catalytic triad, crystal structure, hydrolase fold, *Rhizopus niveus*, triacylglycerol acylhydrolase.

Lipase catalyzes not only the hydrolysis of ester bonds of triacylglycerols but also the synthesis of ester bonds and transesterification. Transesterification by lipases is particularly useful in industry, for example in the production of cocoa butter substitutes (*1*). Because lipase has the unique ability to act at oil-water interfaces, its structure is of particular interest.

Recently, the structures of lipase from various sources have been revealed [*Rhizomucor miehei* (*2-4*), *Rhizopus delemar* (*5, 6*), *Humicola lanuginosa* (*6*), *Geotrichum candidum* (*7, 8*), *Candida rugosa* (*9, 10*), *Candida antarctica* (*11, 12*), *Pseudomonas glumae* (*13*), *Penicillium camembertii* (*14*), human pancreas (*15*), and horse pancreas (*16*)]. Although these lipases are from various sources and often have different amino acid sequences, they do share some common structural properties. First, lipase has a catalytic center which contains a triad of three amino acids (Ser-His-Asp/Glu), like serine proteases such as chymotrypsin and subtilisin (*17*). Second, it has a specific sequence motif; a so-called lipase/esterase consensus sequence (Gly-X-Ser-X-Gly) (*18*). Ser is one of the amino acids in the catalytic center, and this sequence is identical to that in serine proteases. Third, lipase shows an α/β hydrolase fold, which is a common 3-D fold in several other hydrolases (*19*). Moreover, lipase has a so-called flexible lid which shelters the catalytic center in solution in the resting form. In the presence of substrates, lipase has been predicted to undergo conformational change to the active form through movement of the lid and consequent exposure of the catalytic center, based on studies of the structures of complexes of lipases with their inhibitors from *R. miehei* (*20, 21*) and *C. rugosa* (*22*) and of the human pancreatic lipase-procolipase complex (*23-25*).

Lipase from *Rhizopus niveus* shows 1,3 positional specificity more strictly than other lipases. We previously cloned the complementary DNA encoding this lipase to determine its sequence (*26*) and we have reported the purification, characterization, and crystallization of two types of lipase from *R. niveus* (*27*). In addition, we have shown that Lipase II is produced from Lipase I by limited proteolysis through the action of a serine protease that is present in pure Lipase I in a very small amount. In this paper, we describe the crystal structure of Lipase II at a resolution of 2.2 Å. The structure has properties in common with those of other lipases and has an α-helix lid which shelters the catalytic site.

EXPERIMENTAL PROCEDURES

Crystals of Lipase II from *R. niveus*, which was produced by the limited proteolysis of Lipase I, were grown at 20°C by the hanging drop method, as described previously (*28*), with 14-18% polyethylene glycol 8000 in 0.1 M HEPES buffer pH 6.5 as a precipitant and with each drop containing 18 mg/ml protein.

The crystals were tetragonal, and preliminary data are shown in Table I. Native data for a resolution of 2.0 Å and all heavy atom derivative data were collected using the R-AXIS IIc system (Rigaku) with monochromated Cu Kα radiation from a Rigaku RU-200 rotating anode source (Table II). Ten heavy atom derivatives were prepared by a soaking method at a concentration of 0.5-5.0 mM and a soaking time of 1-6 h at 20°C. Heavy atom positions were determined by the standard difference Patterson and

[1] To whom correspondence should be addressed. Tel: +81-297-52-6324, FAX: +81-297-52-6326, E mail: kouno@fujioil.co.jp

Abbreviations: MIR, multiple isomorphous replacement; RmL, *Rhizomucor miehei* lipase; RdL, *Rhizopus delemar* lipase.

difference Fourier methods and were refined using PHASIT from the PHASES software package (W. Furey, VA Medical, and Center and University of Pittsburgh, Pittsburgh, PA). The final heavy atom parameters and statistics are summarized in Table III. The initial multiple isomorphous replacement (MIR) map was unclear because of the low mean figure of merit at a resolution of 2.5 Å. An improvement in the MIR electron density was achieved by applying the solvent flattening technique in the PHASES package. Sixteen cycles of solvent-flattening were carried out. The solvent fraction of the unit cell was set at 37% for the first four cycles, 42% for the next four cycles, and 47% for the final eight cycles. This procedure improved the mean figure of merit to 0.779, and the improved map was clear enough for model building using the TOM modeling graphics package (Bio-Graph, France). Model building was carried out using known amino acid sequence data (*29*) referring to the Cα atomic model of *R. miehei* lipase (RmL) deposited in the Brookhaven Protein Data Bank (PDB) (*30*). The structure was refined using molecular dynamics, energy minimization, and restrained least squares. The first three macrocycles used the slow-cool procedure as implemented in X-PLOR (*31, 32*). The subsequent macrocycles used positional refinement and individual *B*-factor refinement in X-PLOR. After macrocycle refinement, new 2Fo-Fc and Fo-Fc maps were calculated and manual model adjustments were applied using TOM software on an IRIS 4D. Water molecules were added when they appeared as a peak greater than at least three times the standard deviation of the map (3σ) in the Fo-Fc electron-density map and were less than 3.2 Å away from a hydrogen bond acceptor or donor. When the conventional crystallographic *R*-factor had decreased to approximately 0.19, energy minimization was replaced by a restrained least squares minimization, as implemented in the TNT program (*33*).

TABLE I. **Preliminary data for Lipase II crystal.**

Crystal system	Tetragonal
Space group	$P4_3$
Dimensions	$a=b=83.7$, $c=137.9$ Å
	$\alpha=\beta=\gamma=90°$
V ($\times 10^6$ Å^3)	9.7
Crystal density (g/cm^3)	1.16
Solvent content (%)	47
No. of molecules per asymmetric unit	3
V_M (Å^3/Da)	2.5

RESULTS AND DISCUSSION

Lipase II has a unique property as regards crystal growth. In the crystallization of Lipase II from *R. niveus*, pure Lipase I was first obtained (*28*). Lipase I has a characteristic structure consisting of two polypeptide chains [a small peptide with a sugar moiety (A-chain, M_r 7,000) and a large peptide of molecular weight 34,000 (B-chain)] that bind to each other noncovalently. However, in the analysis of the MIR density map, the crystal was found to be Lipase II, which consists of a single polypeptide which lacks the A-chain and 28 N-terminal amino acids of the B-chain of Lipase I. During crystal growth, Lipase I is thought to be converted to Lipase II through limited proteolysis by a small amount of serine protease. Because pure Lipase II could not be crystallized under the same conditions in this case, the presence of the A-chain and the N-terminal amino acids of the B-chain of Lipase I may be required at the start of crystallization to form the nucleus of the Lipase II crystal.

The preliminary crystal data of Lipase II were originally reported to be those of Lipase I. Therefore, those data were recalculated as shown in Table I. The completeness of the data to a resolution of 2.0 to 2.2 Å was less than 80%. So, the data used for model building were those of a resolution from 2.2 to 9.0 Å. Ten heavy atom derivatives were needed

TABLE III. **Statistics of multiple isomorphous replacement.**

	Site	*R* Cullis[a]	*R* Kraut[b]	Phasing power[c]
$Pb(CH_3COO)_2$	4	0.672	0.086	0.96
$UO_2(CH_3COO)_2$	4	0.709	0.147	1.09
$K_3UO_2F_5$	7	0.679	0.125	1.37
$Sm(CH_3COO)_2$	2	0.727	0.116	0.58
Mersalyl	1	0.726	0.078	1.11
CH_3HgCl	3	0.724	0.088	1.10
CH_3HgOH	4	0.896	0.170	0.17
Na_2IrCl_6	7	0.770	0.140	0.44
K_2PtCl_4	2	0.786	0.110	0.41
$K_2Pt(NO_2)_4$	2	0.681	0.145	0.86
Reflection used ($>2\sigma$)		29,925		
Figure of merit		0.568		

[a] R Cullis $=\Sigma\|FPH|_{obs}+/-|FP|_{obs}-|FH|_{obs}|/\Sigma\|FPH|_{obs}+/-|FP|_{obs}|$, where $|FPH|_{obs}$ is the structure factor amplitude of the heavy atom derivatives, $|FP|_{obs}$ is that of the native crystal and $|FH|_{obs}$ is that of the heavy atom. [b] R Kraut $=\Sigma\|FPH|_{obs}-|FPH|_{calc}|/\Sigma|FPH|_{obs}$. [c] Phasing power is the root-mean-square (rms) value of the heavy atom structure factor amplitude ($|FH|_{rms}$) divided by the rms residual lack of closure errors ($|F|_{rms}$) defined as ($|FH|_{rms}/|F|_{rms}$).

TABLE II. **Summary of data collection for native and derivative crystals.**

	Soaking conditions	No. of unique reflections	Resolution limit (Å)	Completeness (%)	merge *R*	Isomorphous differences
Native	—	53,656	2.0	78.0	8.9	—
$Pb(CH_3COO)_2$	2.5 mM, 6 h	28,018	2.5	87.3	9.0	0.091
$UO_2(CH_3COO)_2$	10 mM, 2 h	25,486	2.5	79.4	14.2	0.168
$K_3UO_2F_5$	5 mM, 1 h	28,985	2.5	90.3	14.7	0.162
$Sm(CH_3COO)_2$	2.5 mM, 6 h	27,276	2.5	84.9	10.2	0.121
Mersalyl	1 mM, 2 h	29,399	2.5	91.6	10.0	0.088
CH_3HgCl	0.5 mM, 2 h	29,352	2.5	91.4	13.0	0.103
CH_3HgOH	0.5 mM, 2 h	27,047	2.5	84.2	12.0	0.169
$IrCl_4$	10 mM, 3 h	28,772	2.5	88.8	12.1	0.132
K_2PtCl_4	1 mM, 2 h	27,536	2.5	85.7	10.4	0.105
$K_2Pt(NO_2)_4$	2.5 mM, 2 h	28,684	2.5	89.3	14.8	0.161

for framing the initial MIR density map, even though some of them (CH_3HgOH, Na_2IrCl_6, and K_2PtCl_4) showed a phasing power less than 0.5. The final structure has 6,662 non-hydrogen atoms, including 449 water oxygens. The final *R*-factor for the refined model was 18.6 using 53,656 reflections. In the refined model, 265 amino acid residues, excluding first four residues of one Lipase II molecule, were positioned in the electron map. The three molecules in the crystallographic asymmetric unit are not related by proper symmetry. Average *B*-factors (Cα) of each molecule were 19.0 Å^2 (molecule No. 1), 20.1 Å^2 (molecule No. 2), and 29.7 Å^2 (molecule No. 3). Molecule No. 3 has less interaction with the other molecules in the crystal, so this molecule may have a relatively more flexible structure. Average rms deviations (Cα) were 0.359 Å (molecules No. 1 and No. 2), 0.442 Å (molecules No. 1 and No. 3), and 0.396 Å (molecules No. 2 and No. 3). Molecule No. 3 has a rather high average *B*-factor (Cα), but in this refined molecular model,

TABLE IV. **Refinement statistics of Lipase II.**

No. of amino acid residues	795
No. of water molecules	449
R-factor	18.6
r.m.s. deviation from standard values	
Bond distance (Å)	0.017
Bond angle (deg.)	2.90
B-factor (Å^2)	
Protein	23.0
Solvent	37.2

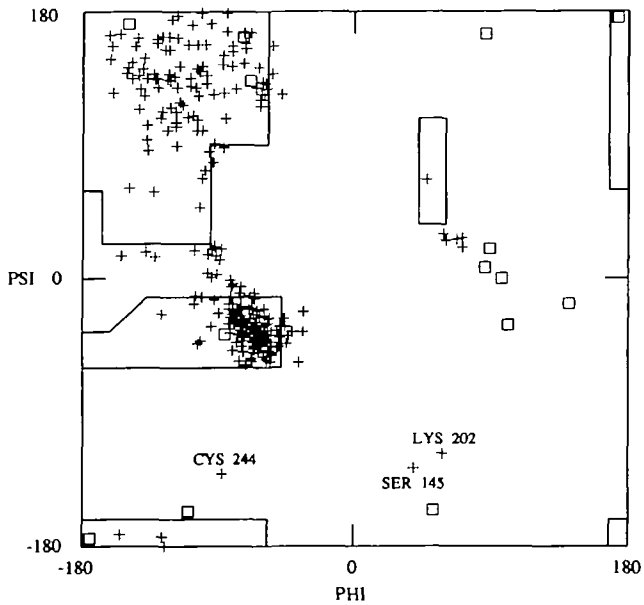

Fig. 1. **The Ramachandran plot for the refined molecular model (molecule No. 1).** Glycine residues are marked with □ and all others are marked with +. The allowed regions of conformational space are shown, and the three non-Gly residues which occur outside these regions are labeled.

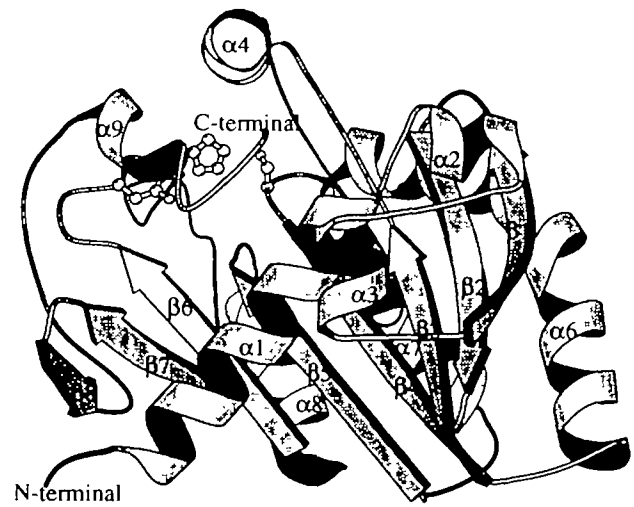

Fig. 2. **Schematic model of the structure of Lipase II generated using MOLSCRIPT (*34*).** The secondary structure has been identified as follows: β-strands: β1, 53-59; β2, 62-70; β3, 74-83; β4, 136-142; β5, 169-176; β6, 194-201; β7, 221-225; β8, 231-236; α-helices: α1, 11-25; α2, 30-36; α3, 41-46; α4, 86-91; α5, 110-119; α6, 121-133; α7, 146-161; α8, 183-192; α9, 253-258. In addition, the catalytic triad is shown in full, and the amino and carboxyl termini are marked.

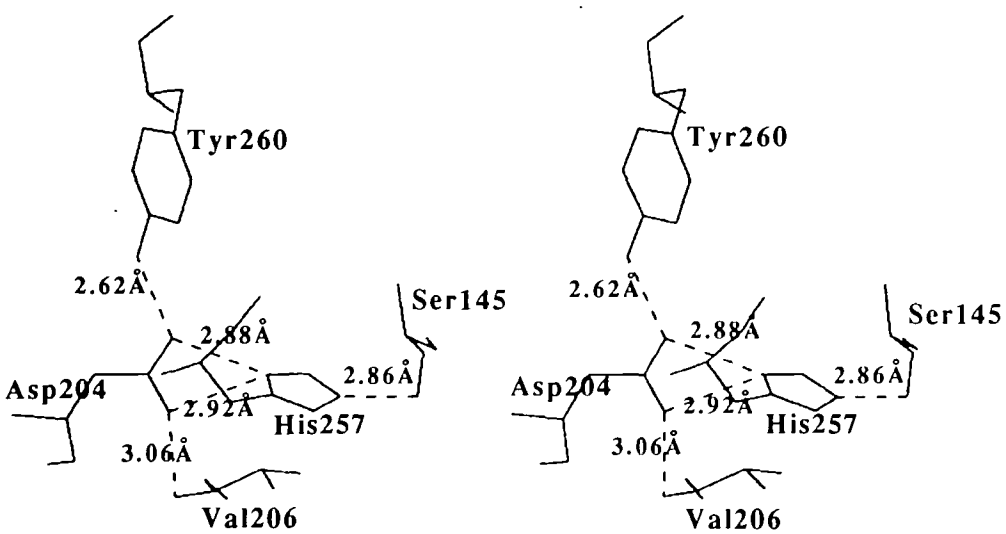

Fig. 3. **Details of the catalytic triad.** The catalytic triad residues (Ser145, Asp204, and His257) and two residues which stabilize Asp204 (Val206 and Tyr260) are shown in solid lines. Dashed lines represent hydrogen bonds between their side-chain atoms. The length of each hydrogen bond is shown for clarity.

it is almost identical with the other molecules. Table IV shows the statistics for the refined model. The mean error in the model estimated from the Luzzati plot suggests a maximum average error of less than 0.3 Å (data not shown). In the Ramachandran plot (Fig. 1), three non-Gly residues (Ser145, Lys202, Cys244) are outside the energetically suitable regions. These residues are well-defined on the electron density maps. The disposition of Ser145 (ϕ, 39°; ψ, −127°) in these distinctive areas is discussed later. Lys202 (ϕ,58°; ψ, −117°) is located at the end of a β-strand (residues 194-201) and is in the $i+1$ position of a distorted type 1 turn. Cys244 (ϕ, −87°; ψ, −131°) forms a disulfide bond with Cys235.

The secondary structure of Lipase II consists of nine α-helices and eight β-strands. These eight β-strands are arranged in sequence and in parallel but are slightly wound

TABLE V. **Main chain conformational angles around active serine in Lipase II and RmL.**[a]

Residue	Lipase II			RmL		
	ϕ	ψ	R[c]	ϕ	ψ	R
Gly	173	176	n	−172	146	β
X	−124	163	β	−105	144	β
Ser	39	−128	ε	62	−121	ε
X	−64	−21	α	−57	−39	α
G/A[b]	−72	−15	α	−56	−35	α

[a]The value for RmL is extracted from the Protein Data Bank. [b]G/A: Glycine corresponds to the amino acid of Lipase II and alanine corresponds to that of RmL. [c]R: The regions of the conformation space favoring phi-psi combination in the Ramachandran plot. Abbreviations are meanig as follows: α, allowed alpha helix; β, allowed beta sheet; ε, allowed epsilon positions; n, not allowed for non-glycine residues.

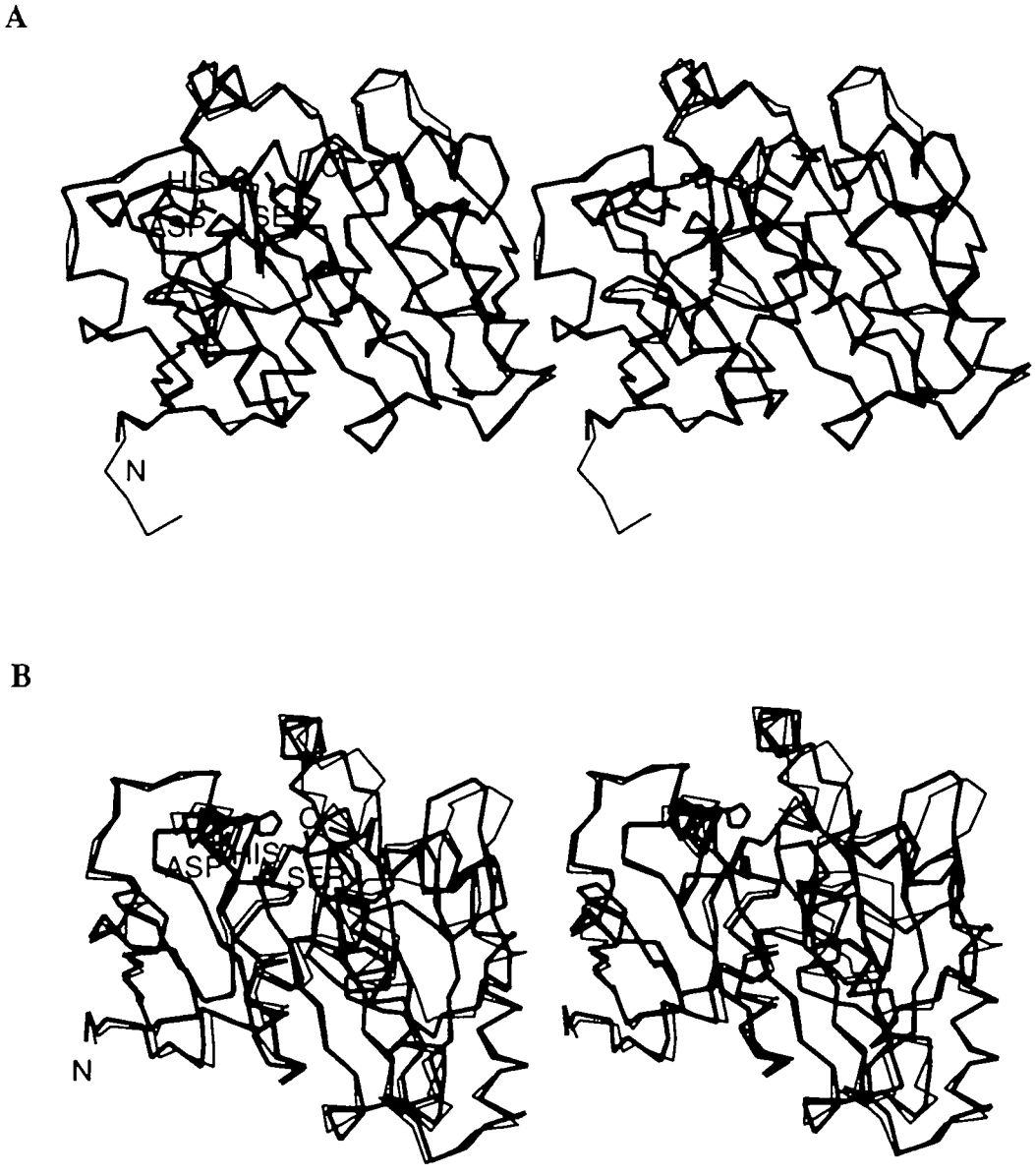

Fig. 4. **A structural comparison of Lipase II, RdL and RmL.** A: A stereo diagram showing the superposition of Lipase II (thick line) and RdL (thin line); the Cα atoms only and the catalytic triad of Lipase II are shown. N and C indicate the amino and carboxyl termini of Lipase II. B: A diagram of Lipase II (thick line) and RmL (thin line); details as in A.

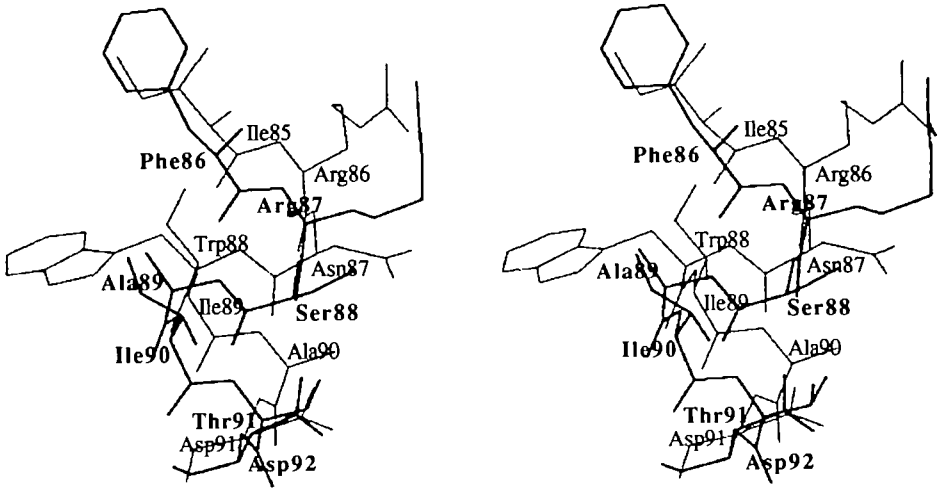

Fig. 5. **A comparison of lids between Lipase II and RmL.** The predicted lid of Lipase II (residues 86-92) is shown by thicker lines, and the lid of RmL (residues 85-91) is shown by thinner lines.

(Fig. 2). The first of the eight α-helices passes across one side of the parallel β-strands, while on the other side it interacts with many loops and turns. Three disulfide bonds (residues 29-268, 40-43, and 235-244) stabilize the molecule.

It has been shown that the catalytic center consists of a triad of three amino acids (Ser145, Asp204, and His257) based on a comparison of a sequence analysis of cDNA encoding *R. niveus* lipase (*26*) and the tertiary structure of RmL (*2*). These three amino acids interact through hydrogen bonds in their side chains, as shown in Fig. 3. The O^{γ} of Ser145 bonds to $N^{\epsilon 2}$ of His257, and $N^{\delta 1}$ of the imidazole group (His257) bonds to $O^{\delta 1}$ of Asp204. The carboxyl oxygen atoms of Asp204 form hydrogen bonds with O^{η} of Tyr260 and the main-chain N of Val206 to stabilize the aspartic acid. Catalytic serine (Ser145) is located outside the energetically suitable region as stated above. However, the disposition of this residue is similar to that of the serine which forms the active center of serine proteinases and other lipases. Lipase II has a so-called consensus sequence, Gly-X-Ser-X-Gly, like serine proteinases and other lipases (*18*). The oxyanion hole is presumably formed in the active species by the hydroxyl and main chain amide groups of Thr83. However, it has been suggested that lipases and wheat carboxypeptidase exhibit a secondary structure very different from that of serine proteinases (*35*).

Lipase II has a catalytic center conformation similar to that of RmL, except for glycine in position 1 (Table V). In addition, the structure around the active center resembles the structure in lipases known as the α/β hydrolase fold (*19*); the consensus pentapeptide forms a β-ϵSer-α motif (*36*), which consists of a sharp turn at the active serine that connects a β-sheet and an α-helix. The catalytic center of Lipase II is buried in the molecule, as in other lipases. In general, lipases have an α-helix lid which covers the catalytic center. In Lipase II, an α-helix (helix No. 4; Phe86-Asp92) is in a position where it can shelter the catalytic triad. It is believed that this α-helix forms a lid, which moves to expose the catalytic center in the presence of substrates, based on a comparison with the conformation of RmL.

Lipase II has structural properties that are found in other lipases. In particular, the degree of identity of Lipase II and RmL is 55.7% in the primary structure and that of Lipase II and *R. delemar* lipase (RdL) is 100%. The overall structures of Lipase II, RdL and RmL all resemble each other. RmL and RdL (molecule A) are lacking in the first four amino acid residues in their electron density maps, as is Lipase II. So, it is suggested that these residues are conformationally unstable in solution. The coordinates of RdL deposited in the Brookhaven Protein Data Bank cover only the Cα atoms. So, we can not compare Lipase II with RdL in detail. Lipase II and RmL show similar secondary structures and disulfide bonds. However, the average rms (Cα) of the same amino acids in the primary structures of Lipase II (molecule No. 1) and RmL is 0.750 Å and that of Lipase II and RdL (molecule B) is 0.581 Å. These value are high, and it is implied that the details of the tertiary structure of Lipase II are different from those of RmL and RdL (Fig. 4).

In RdL, the conformation of the lid is heterogeneous (*6*). The asymmetric unit of the RdL crystals contains two molecules which have different conformations owing to a combination of the effects of the protein-detergent interaction with the crystal contacts. The lid of one molecule is in the expected closed conformation blocking the active site (molecule B), while that of another molecule is in the intermediate position between the closed one and the open one (molecule A). The conformation of the lid of Lipase II resembles that of the closed form of RdL molecule B. The presence of detergent during the crystallization of RdL presumably has an effect on the packing of the crystal. There is no detergent in the crystal of Lipase II. Consequently, although the identity in primary structure between Lipase II and RdL is 100%, some differences at the molecular surface exist between Lipase II and RdL (Fig. 4A).

The structure of the lid in Lipase II differs from that in RmL (Fig. 5). In the lid of RmL, Arg86 has been shown to stabilize the active form (*37*), and Trp88 undergoes a significant change to expose the hydrophobic area and blocks the position which the inhibitor (the analog for the substrate) occupies in the complex (*21*). In these positions of Lipase II, arginine is preserved as Arg87, but tryptophan is replaced by Ala89. Alanine is a smaller amino acid than tryptophan. Moreover, the tetrapeptide which interacts with the lid in the open form (Tyr-Asp-Thr-Asn in RmL) is different among the lipases. At the N-terminal amino acid

(Tyr60) of the tetrapeptide of RmL, the carbonyl group bonds the polar side chain of Asn87 in the lid (*21*). In Lipase II, tyrosine and asparagine are replaced by Ser61 and Ser88, respectively. These replacements be related to the difference in specific activity between Lipase II and RmL [Lipase II, 6,200 U/mg protein (*27*); RmL, 1,900 U/mg protein (*38*)]. So, it is expected that the open form of Lipase II is different from that of RmL.

The coordinates of Lipase II will be deposited in the Brookhaven Protein Data Bank. Further, we have recently crystallized the complex of Lipase II with its inhibitor and Lipase I. We hope to elucidate the active form of Lipase II and the role of the A-chain of Lipase I.

REFERENCES

1. Matsuo, T., Sawamura, N., Hashimoto, Y., and Hashida, W. (1980) Method for producing a cacao butter substitute. *UK Patent*, GB 2035359 B
2. Brady, L., Brozozowski, A.M., Derewenda, Z.S., Dodson, E., Dodson, G., Tolley, S., Turkenberg, J.P., Christiansen, L., Huge-Jensen, B., Novskov, L., Thim, L., and Menge, U. (1990) A serine protease triad forms the catalytic centre of a triacylglycerol lipase. *Nature* **343**, 767-770
3. Derewenda, Z.S., Derewenda, U., and Dodson, G.G. (1992) The crystal and molecular structure of the *Rhizomucor miehei* triacylglycerol lipase at 1.9 Å resolution. *J. Mol. Biol.* **227**, 818-839
4. Brozozowski, A.M., Derewenda, Z.S., Dodson, E.J., Dodson, G.G., and Turkenberg, J.P. (1992) Structure and molecular model refinement of *Rhizomucor miehei* triacylglyceride lipase: A case study of the use of simulated annealing in partial model refinement. *Acta Crystallogr.* **B48**, 307-319
5. Swenson, L., Green, R., Joerger, R., Haas, M., Scott, K., Wei, Y., Derewenda, U., Lawson, D.M., and Derewenda, Z.S. (1994) Crystallization and preliminary crystallographic studies of the precursor and mature forms of a neutral lipase from the fungus *Rhizopus delemar*. *Proteins* **18**, 301-306
6. Derewenda, U., Swenson, L., Wei, Y., Green, R., Kobos, P.M., Joerger, R., Haas, M.J., and Derewenda, Z.S. (1994) Conformational lability of lipases observed in the absence of an oil-water interface: Crystallographic studies of enzymes from the *Humicola lanuginosa* and *Rhizopus delemar*. *J. Lipid Res.* **35**, 524-534
7. Schrag, J.D., Li, Y., Wu, S., and Cygler, M. (1991) Ser-His-Glu triad forms the catalytic site of the lipase from *Geotrichum candidum*. *Nature* **351**, 761-764
8. Schrag, J.D. and Cygler, M. (1993) 1.8 Å refined structure of the lipase from *Geotrichum candidum*. *J. Mol. Biol.* **230**, 575-591
9. Grochulski, P., Li, Y., Schrag, J.D., Bouthillier, F., Smith, P., Harrison, D., Rubin, B., and Cygler, M. (1993) Insights into interfacial activation from an open structure of *Candida rugosa* lipase. *J. Biol. Chem.* **268**, 12843-12847
10. Grochulski, P., Li, Y., Schrag, J.D., and Cygler, M. (1994) Two conformational states of *Candida rugosa* lipase. *Protein Sci.* **3**, 82-91
11. Uppenberg, J., Patkar, S., Bergfors, T., and Jones, T.A. (1994) Crystallization and preliminary X-ray studies of lipase B from *Candida antarctica*. *J. Mol. Biol.* **235**, 790-792
12. Uppenberg, J., Hansen, M.T., Patkar, S., and Jones, T.A. (1994) The sequence, crystal structure determination and refinement of two crystal forms of lipase B from *Candida antarctica*. *Structure* **2**, 293-308
13. Noble, M.E.M., Cleaby, A., Johnson, L.N., Egmond, M.R., and Frenken, L.G.J. (1993) The crystal structure of triacylglycerol lipase from *Pseudomonas glumae* reveals a partially redundant catalytic aspartate. *FEBS Lett.* **331**, 123-128
14. Derewenda, U., Swenson, L., Green, R., Wei, Y., Yamaguchi, S., Haas, M.J., and Derewenda, Z.S. (1994) An unusual buried polar cluster in a family of fungal lipases. *Struct. Biol.* **1**, 36-47
15. Winkler, F.K., D'Arcy, A., and Hunziker, W. (1990) Structure of human pancreatic lipase. *Nature* **343**, 771-774
16. Bourne, Y., Martinez, C., Kerfelec, B., Lombardo, D., Chapus, C., and Cambillau, C. (1994) Horse pancreatic lipase: The crystal structure refined at 2.3 Å resolution. *J. Mol. Biol.* **238**, 709-732
17. Blow, D.M., Birktoft, J., and Hartly, B. (1969) Role of a buried acid group in the mechanism of action of chymotrypsin. *Nature* **221**, 337-339
18. Brenner, S. (1988) The molecular evolution of genes and proteins: A tale of two serines. *Nature* **334**, 528-530
19. Ollis, D.L., Cheah, E., Cygler, M., Dijkstra, B., Frolow, F., Franken, S.M., Harel, M., Remington, S.J., Silman, I., Schrag, J., Sussman, J.L., Verschueren, K.H.G., and Goldman, A. (1992) The α/β hydrolase fold. *Protein Eng.* **5**, 197-211
20. Brozozowski, A.M., Derewenda, U., Derewenda, Z.S., Dodson, G.G., Lawson, D.M., Turkenberg, J.P., Bjorkling, F., Huge-Jensen, B., Patkar, S.A., and Thim, L. (1991) A model for interfacial activation in lipases from the structure of a fungal lipase-inhibitor complex. *Nature* **351**, 491-494
21. Derewenda, U., Brozozowski, A.M., Lawson, D.M., and Derewenda, Z.S. (1992) Catalysis at the interface: The anatomy of a conformational change in a triglyceride lipase. *Biochemistry* **31**, 1532-1541
22. Grochulski, P., Bouthillier, F., Kazlauskas, R.J., Serreqi, A.N., Schrag, J.D., Ziomek, E., and Cygler, M. (1994) Analogs of reaction intermediates identify a unique substrate binding site in *Candida rugosa* lipase. *Biochemistry* **33**, 3494-3500
23. Tilbeurgh, H.V., Sarda, L., Verger, R., and Cambillau, C. (1992) Structure of the pancreatic lipase-procolipase complex. *Nature* **359**, 159-162
24. Tilbeurgh, H.V., Gargouri, Y., Dezam, C., Egloff, M.P., Nesa, M.P., Ruganie, N., Sarda, L., Verger, R., and Cambillau, C. (1993) Crystallization of pancreatic procolipase and of its complex with pancreatic lipase. *J. Mol. Biol.* **229**, 552-554
25. Tilbeurgh, H.V., Egloff, M.P., Martinez, C., Pugani, N., Verger, R., and Cambillau, C. (1993) Interfacial activation of the lipase-procolipase complex by mixed micelles revealed by X-ray crystallography. *Nature* **362**, 814-820
26. Kugimiya, W., Ohtani, Y., Kohno, M., and Hashimoto, Y. (1992) Cloning and sequence analysis of cDNA encoding *Rhizopus niveus* lipase. *Biosci. Biotech. Biochem.* **56**, 716-719
27. Kohno, M., Kugimiya, W., Hashimoto, Y., and Morita, Y. (1994) Purification, characterization and crystallization of two types of lipase from *Rhizopus niveus*. *Biosci. Biotech. Biochem.* **58**, 1007-1012
28. Kohno, M., Kugimiya, W., Hashimoto, Y., and Morita, Y. (1993) Preliminary investigation of crystal of Lipase I from *Rhizopus niveus*. *J. Mol. Biol.* **229**, 785-786
29. Boel, E., Huge-Jensen, B., Christensen, M., Thim, L., and Fiil, N.P. (1988) *Rhizomucor miehei* triglyceride lipase is synthesized as a precursor. *Lipids* **23**, 701-706
30. Bernstein, F.C., Koetzle, T.F., Williams, G.J.B., Meyer, E.F., Jr., Brice, M.D., Rodgers, J.R., Kennard, O., Shimanouchi, T., and Tasumi, M. (1977) The Protein Data Bank: A computer-based archival file for macromolecular structures. *J. Mol. Biol.* **112**, 535-542
31. Brunger, A.T. (1992) *X-PLOR Version 3.1 Manual: A System for Crystallography and NMR*, Yale University Press, New Haven, CT
32. Brunger, A.T., Kuriyan, J., and Karplus, M. (1987) Crystallographic R factor refinement by molecular dynamics. *Science* **35**, 458-460
33. Tronrud, D.E., Ten Eyck, L.F., and Mathews, B.W. (1988) An efficient-purpose least-squares refinement program for macromolecular structures. *Acta Crystallogr.* **A43**, 489-501
34. Kraulis, P.J. (1991) MOLSCRIPT: A program to produce both detailed and schematic plots of protein structures. *J. Appl. Crystallogr.* **24**, 946-950
35. Derewenda, Z.S. (1994) Structure and function of lipases. *Adv. Protein Chem.* **45**, 1-52
36. Derewenda, Z.S. and Derewenda, U. (1991) Relationships among serine hydrolases: Evidence for a common structural motif in triacylglyceride lipases and esterases. *Biochem. Cell Biol.* **69**, 842-851
37. Holmquist, M., Norin, M., and Hult, K. (1993) The role of arginines in stabilizing the active open-lid conformation of *Rhizomucor miehei* lipases. *Lipids* **28**, 721-726
38. Huge-Jensen, B., Galluzzo, D.R., and Jensen, R.G. (1987) Partial purification and characterization of free and immobilized lipases from *Mucor miehei*. *Lipids* **22**, 559-565